Electronic Supplementary Material (ESI) for Polymer Chemistry.
This journal is © The Royal Society of Chemistry 2021

Supporting Information

Organocatalytic Sequential Ring-Opening Polymerization of Cyclic Ester/Epoxide and *N*-Sulfonyl Aziridine: Metal-Free and Easy Access to Block Copolymers

*Huishan Huang, Wenyi Luo, Linlin Zhu, Ying Wang and Zhen Zhang**

Scheme S1. (a) Phenylmethanol initiated ROP of TsMAz using succinic anhydride; (b) failed sequential ROP of ε-caprolactone and TsMAz using succinic anhydride; (c) failed phenylmethanol initiated ROP of TsMAz using *n*-hexyl isocyanate.

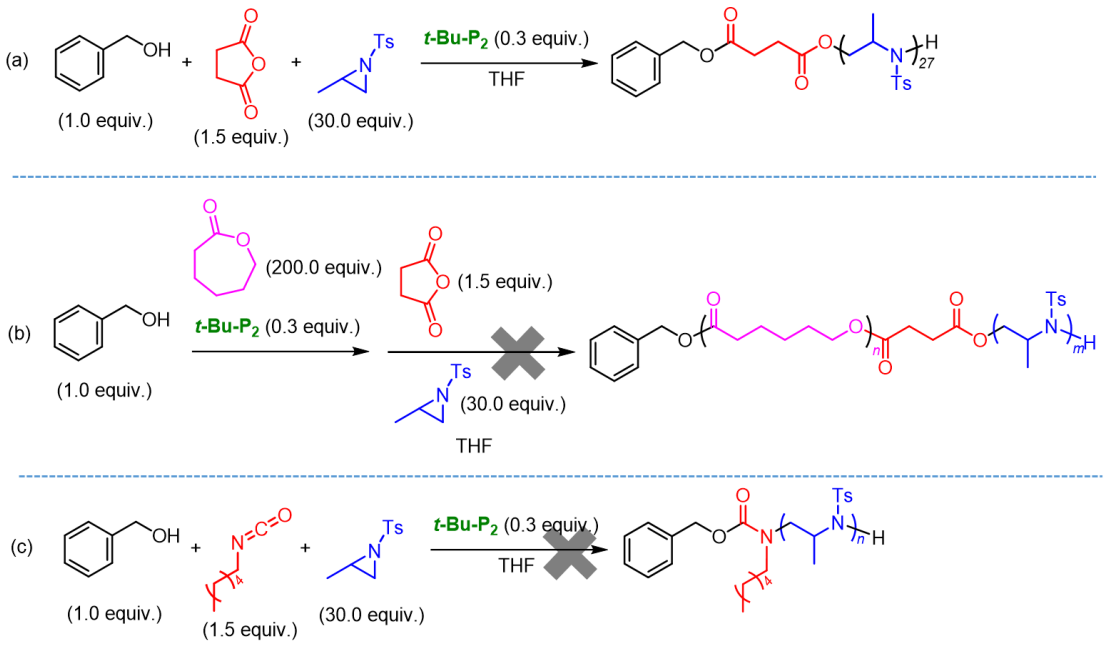

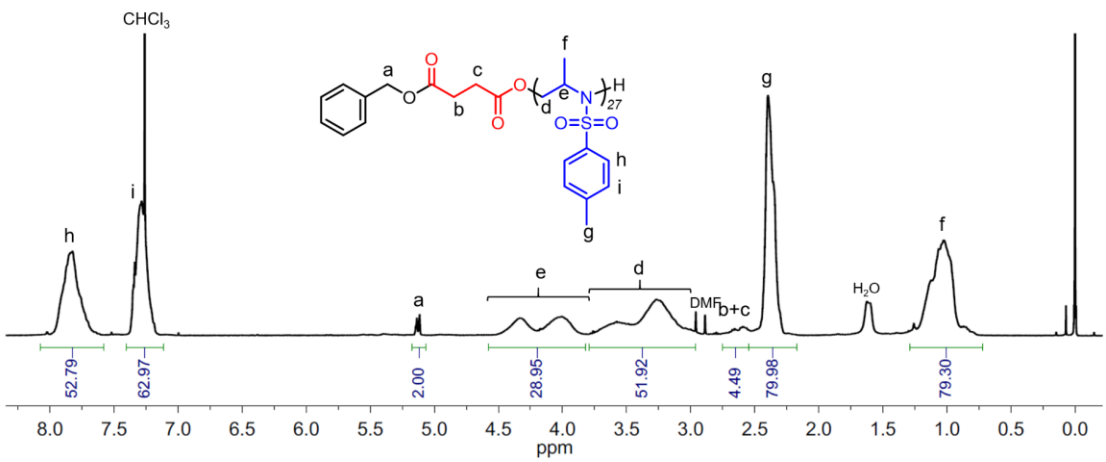

Figure S1. ^{1}H NMR ($CDCl_3$, 400 MHz) spectrum of $P(TsMAz)_{27}$ (sample of Scheme S1a).

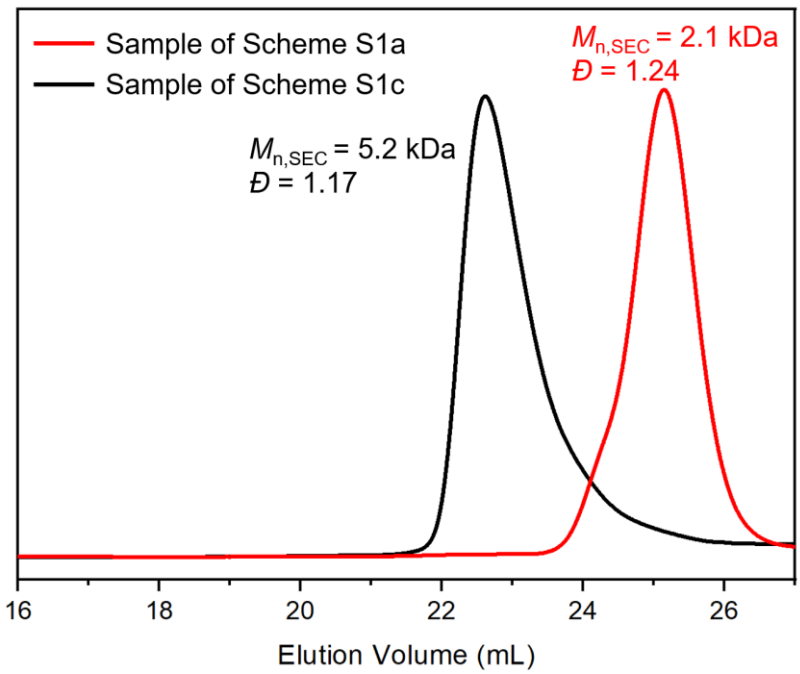

Figure S2. SEC traces (THF, 35 °C) of samples synthesized in Scheme S1a & c.

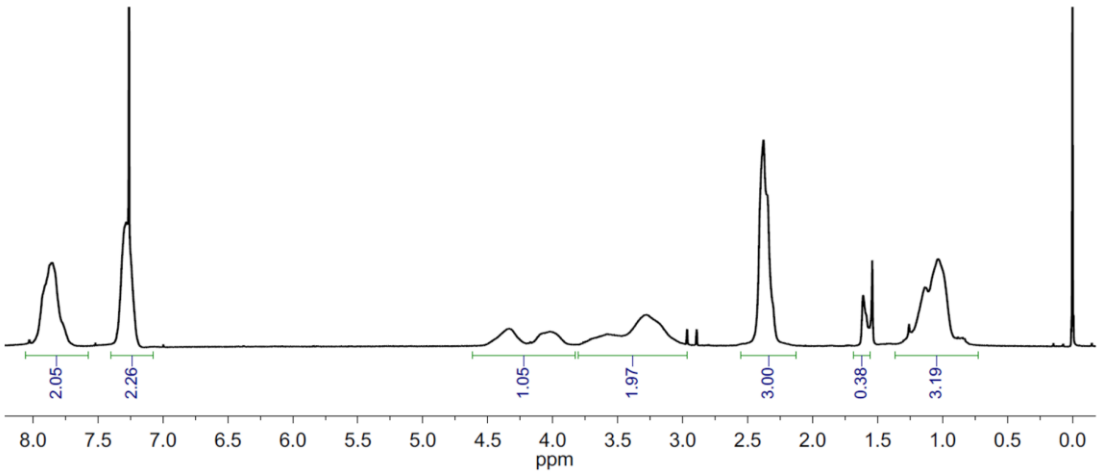

Figure S3. ^{1}H NMR ($CDCl_3$, 400 MHz) spectrum of P(TsMAz) (sample of Scheme S1c).

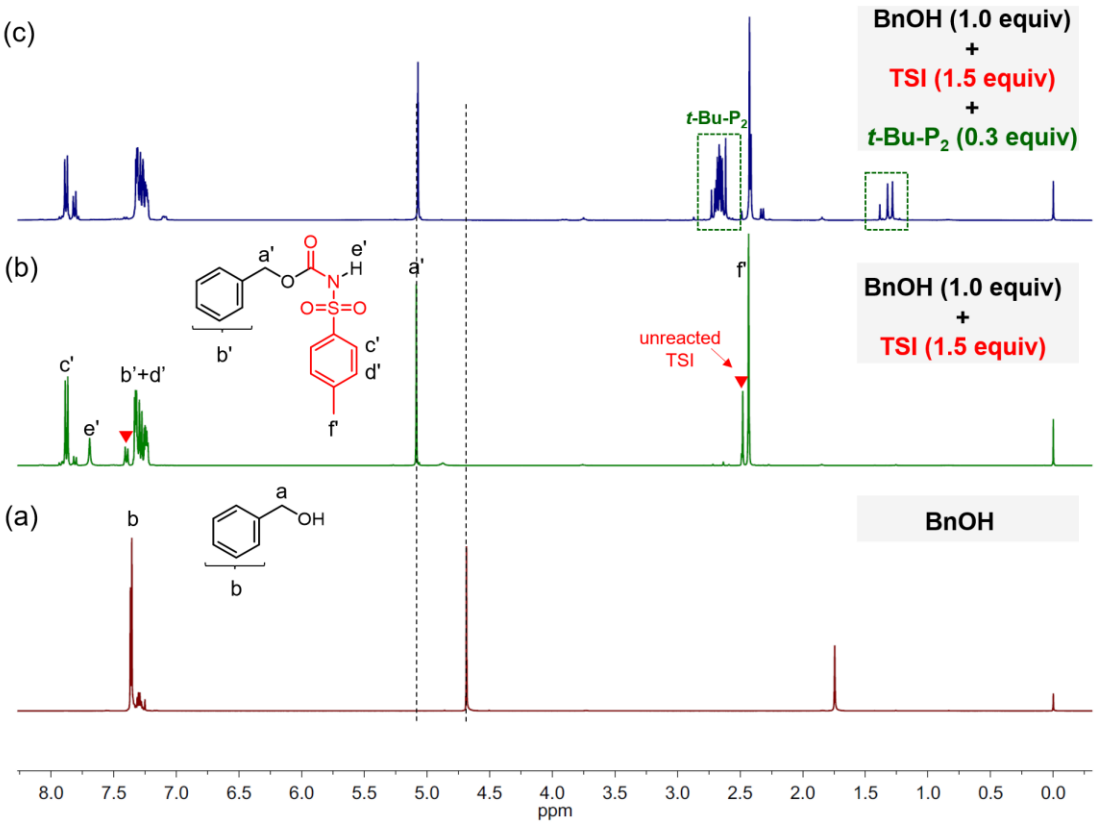

Figure S4. ^{1}H NMR (400 MHz, $CDCl_3$) spectra of (a) phenylmethanol (BnOH); (b) a mixture of BnOH (1.0 equiv), and TSI (1.5 equiv) in $CDCl_3$; (c) a mixture of BnOH (1.0 equiv), TSI (1.5 equiv), and *t*-Bu-P_2 (0.3 equiv) in $CDCl_3$. The mixtures b & c were prepared and kept for ~5 minutes at room temperature, then measured by ^{1}H NMR analysis. Benzyl tosylcarbamate was formed in the mixture b & c. Benzyl tosylcarbamate: ^{1}H NMR ($CDCl_3$, 400 MHz): δ 2.43 (3H, s), 5.08 (3H, s), 7.23-7.26 (2H, m), 7.29 (2H, d, J = 8.0 Hz), 7.32-7.33 (3H, m), 7.69 (1H, bs), 7.88 (2H, d, J = 8.0 Hz). This data agrees with that reported previously (Ref. *J. Am. Chem. Soc.* **2009**, *131*, 33, 11701–11706).

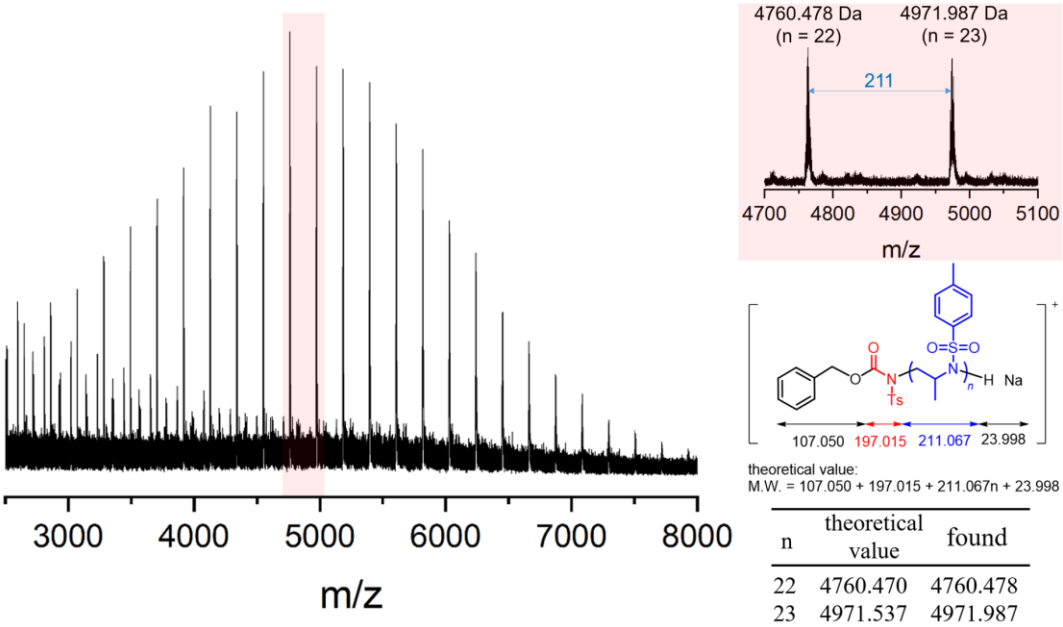

n	theoretical value	found
22	4760.470	4760.478
23	4971.537	4971.987

Figure S5. MALDI-ToF MS of P(TsMAz) (sample of entry 1, Table 1).

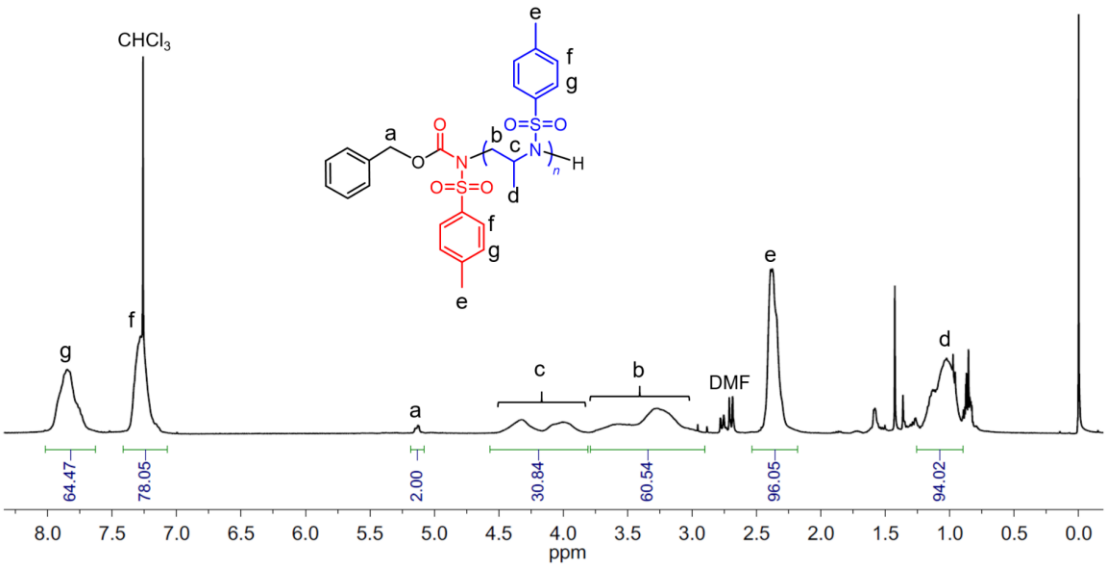

Figure S6. ^{1}H NMR (400 MHz, $CDCl_3$) spectrum of P(TsMAz) (sample of entry 1, Table 1). The molar mass determined by end-group analysis was calculated as follows: $M_{n,NMR} = MW_{BnOH} + MW_{TSI} + MW_{TsMAz} \times (I_c/I_a \times 2)$, I_c: the integral of signal c, I_a: the integral of signal a.

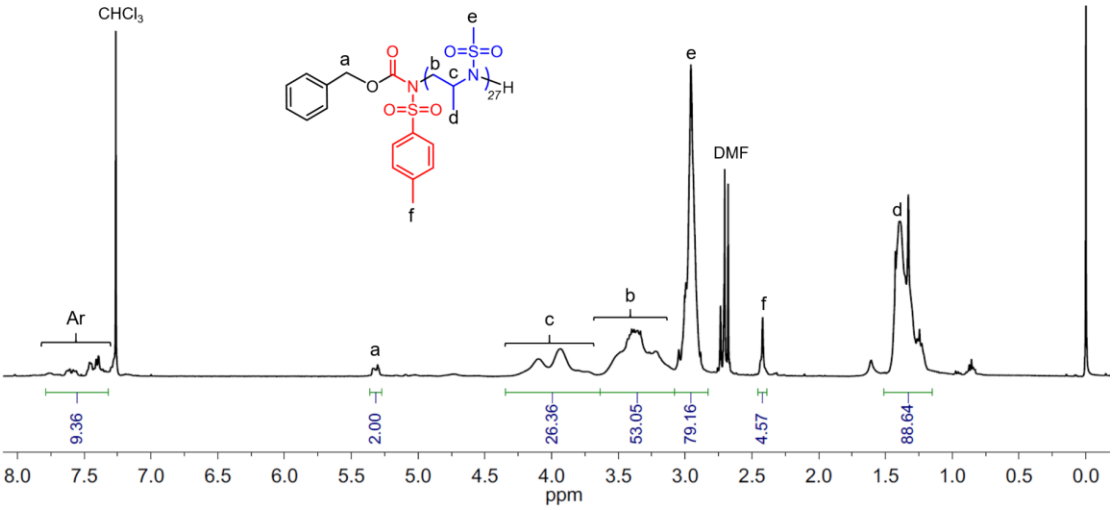

Figure S7. ^{1}H NMR (400 MHz, $CDCl_3$) spectrum of P(MsMAz) (sample of entry 2, Table 1). The molar mass determined by end-group analysis was calculated as follows: $M_{n,NMR} = MW_{BnOH} + MW_{TSI} + MW_{MsMAz} \times (I_c/I_a \times 2)$, I_c: the integral of signal c, I_a: the integral of signal a.

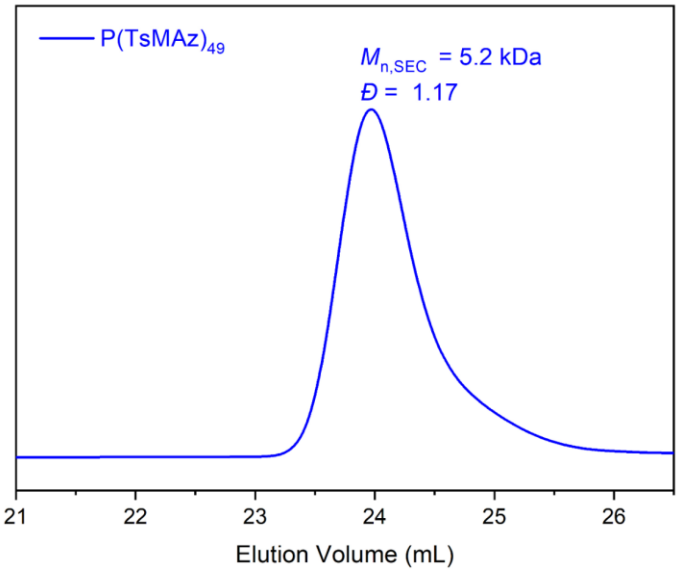

Figure S8. SEC traces (THF, 35 °C) of $P(TsMAz)_{49}$ (sample of entry 3, Table 1).

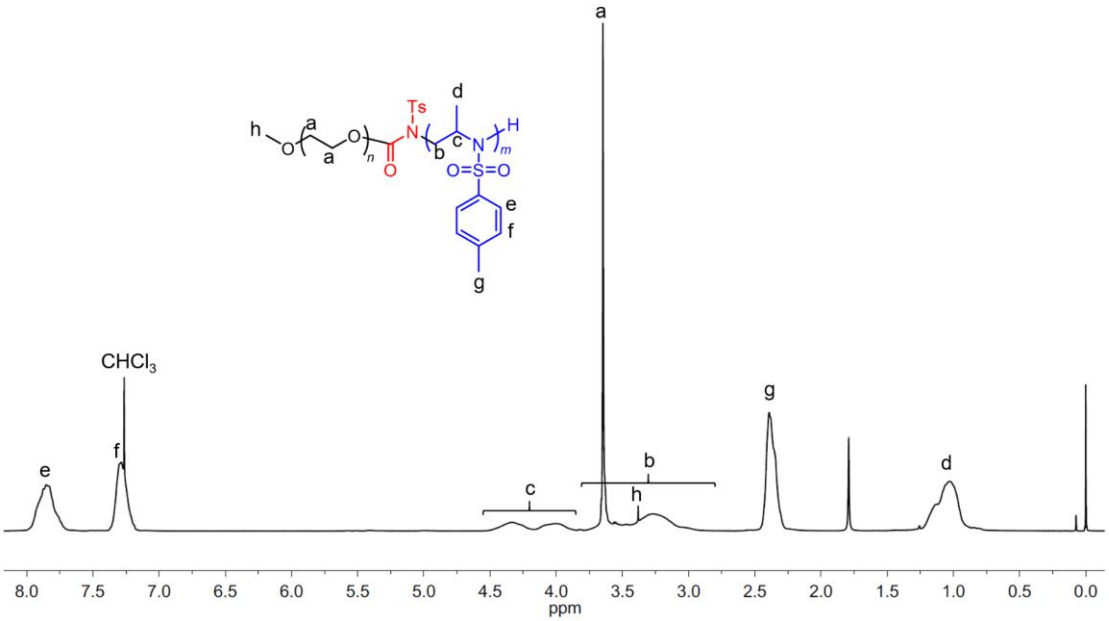

Figure S9. ^{1}H NMR (400 MHz, $CDCl_3$) spectrum of P(TsMAz) (sample of entry 4, Table 1). $M_{n,NMR}$ was not determined due to the overlap of signals h and b.

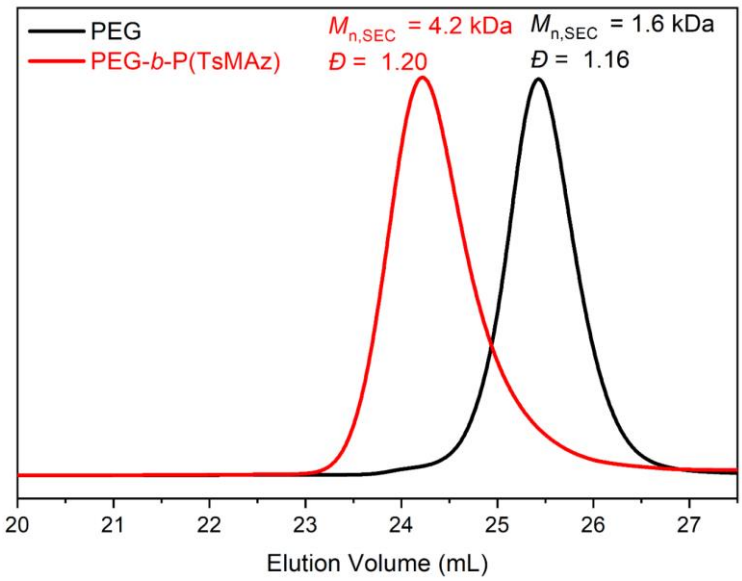

Figure S10. SEC traces (THF, 35 °C) of PEG and PEG-*b*-P(TsMAz) (sample of entry 4, Table 1).

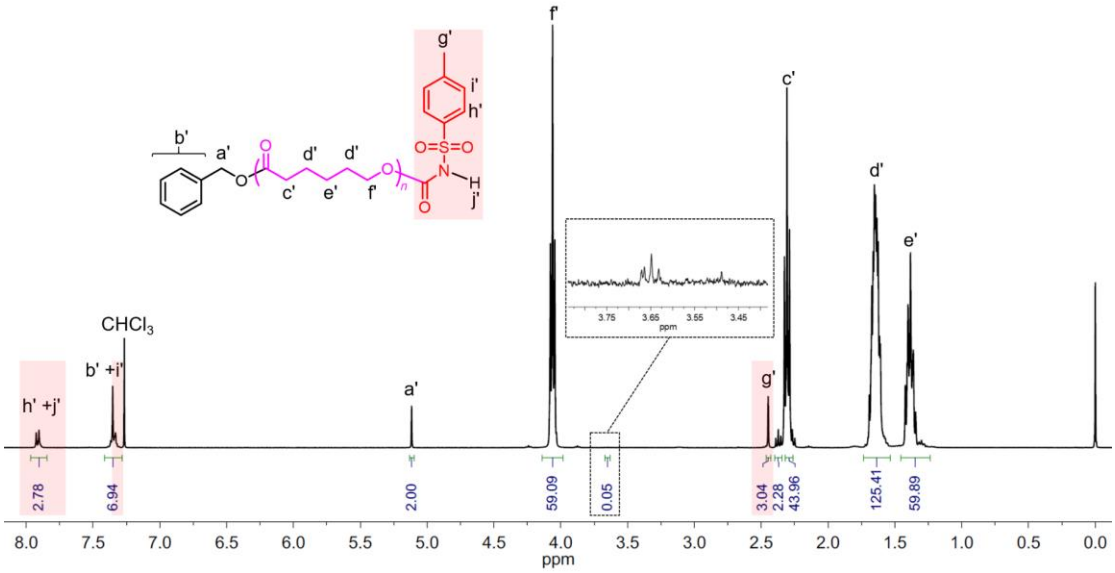

Figure S11. ^{1}H NMR (400 MHz, $CDCl_3$) spectrum of ω-NHTs PCL.

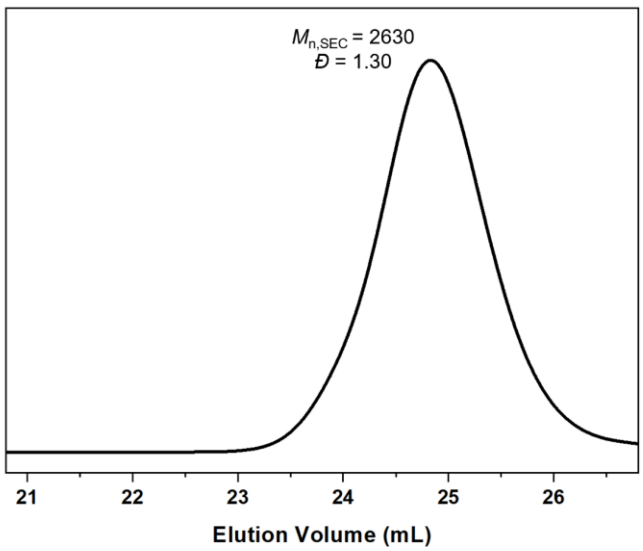

Figure S12. SEC traces (THF, 35 °C) of ω-NHTs PCL.

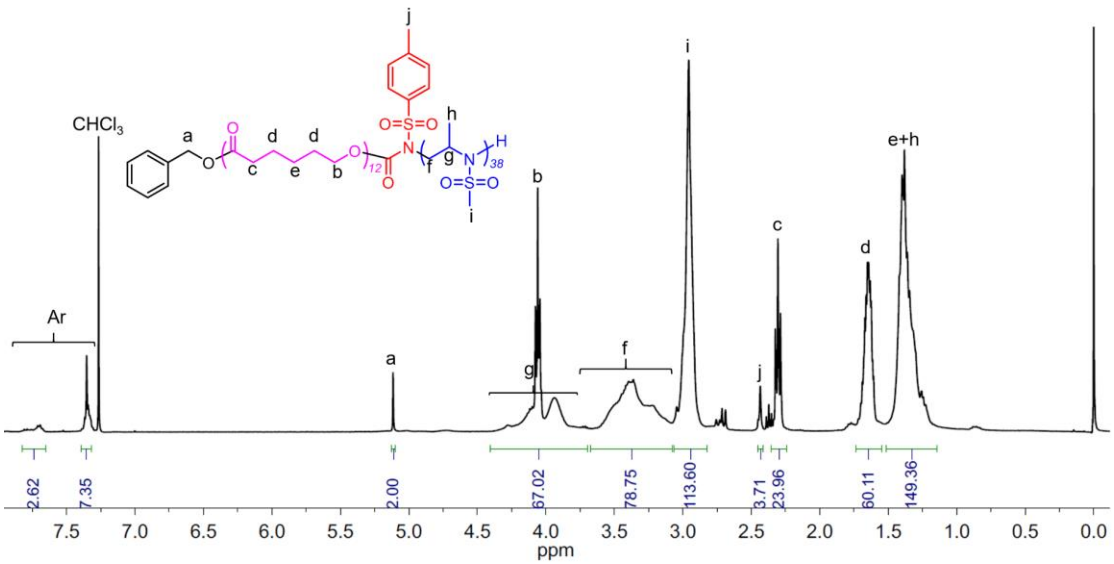

Figure S13. ^{1}H NMR (400 MHz, $CDCl_3$) spectrum of PCL_{12}-*b*-P(MsMAz)$_{38}$ (sample of entry 3, Table 2). The molar mass determined by end-group analysis was calculated as follows: $M_{n,NMR} = MW_{BnOH} + MW_{TSI} + MW_{CL} \times (I_d/I_a \times 2)/4 + MW_{MsMAz} \times (I_f/I_a \times 2)/2$, I: the integral of the related signal.

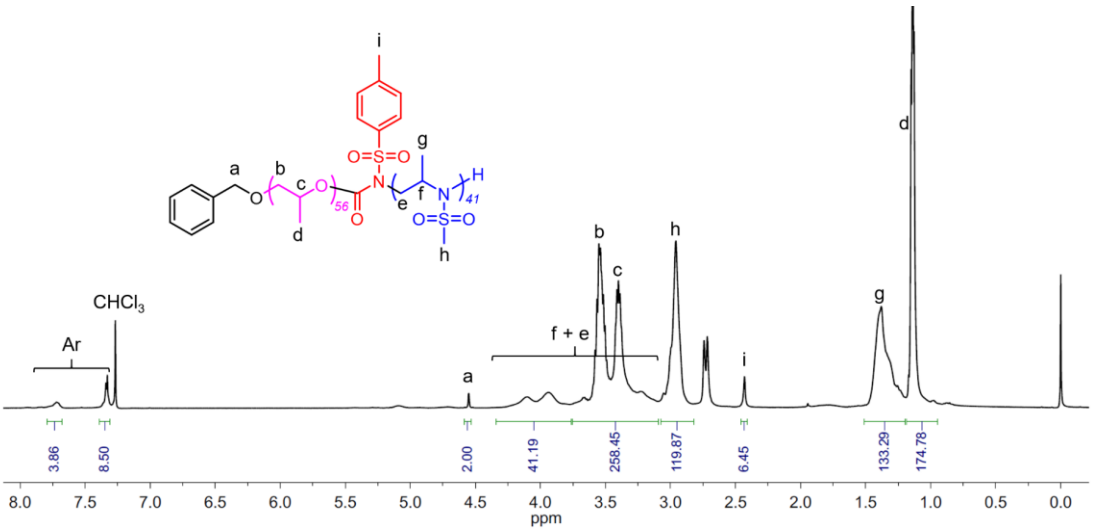

Figure S14. ^{1}H NMR (400 MHz, $CDCl_3$) spectrum of PPO_{56}-*b*-P(MsMAz)$_{41}$ (sample of entry 6, Table 2). The molar mass determined by end-group analysis was calculated as follows: $M_{n,NMR} = MW_{BnOH} + MW_{TSI} + MW_{PO} \times (I_d/I_a \times 2)/3 + MW_{MsMAz} \times (I_g/I_a \times 2)/3$, I: the integral of the related signal.

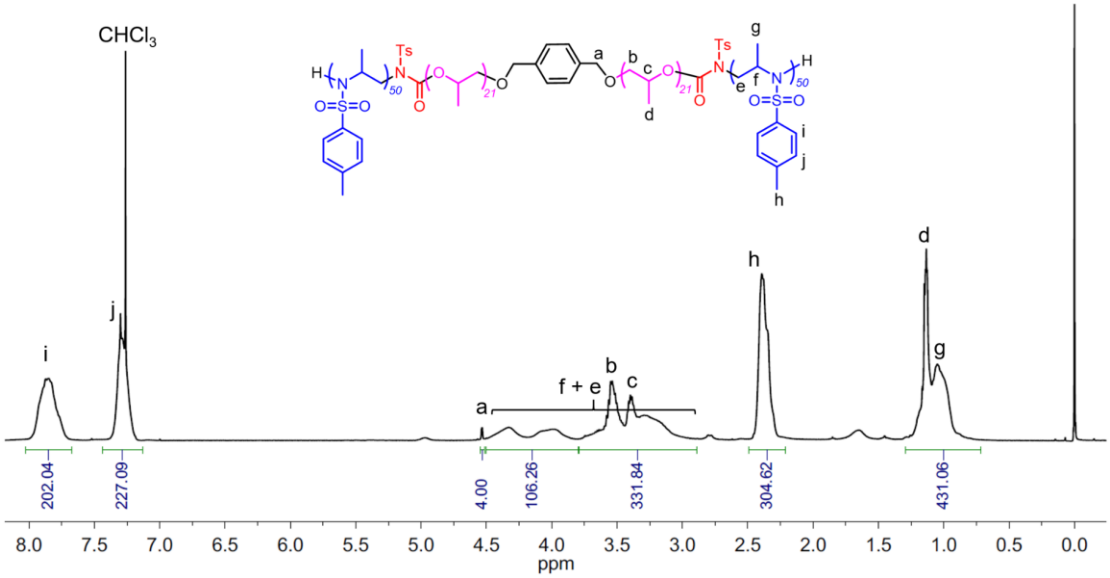

Figure S15. ^{1}H NMR (400 MHz, $CDCl_3$) spectrum of P(TsMAz)$_{50}$-*b*-PPO$_{42}$-*b*-P(TsMAz)$_{50}$ (sample of entry 7, Table 2). The molar mass determined by end-group analysis was calculated as follows: $M_{n,NMR}$ = $MW_{initiator}$ + MW_{TSI} ×2 + MW_{PO} × [(I_d + I_g – I_h)/I_a × 4]/3 + MW_{TsMAz} × (I_h/I_a × 4)/3, *I*: the integral of the related signal.

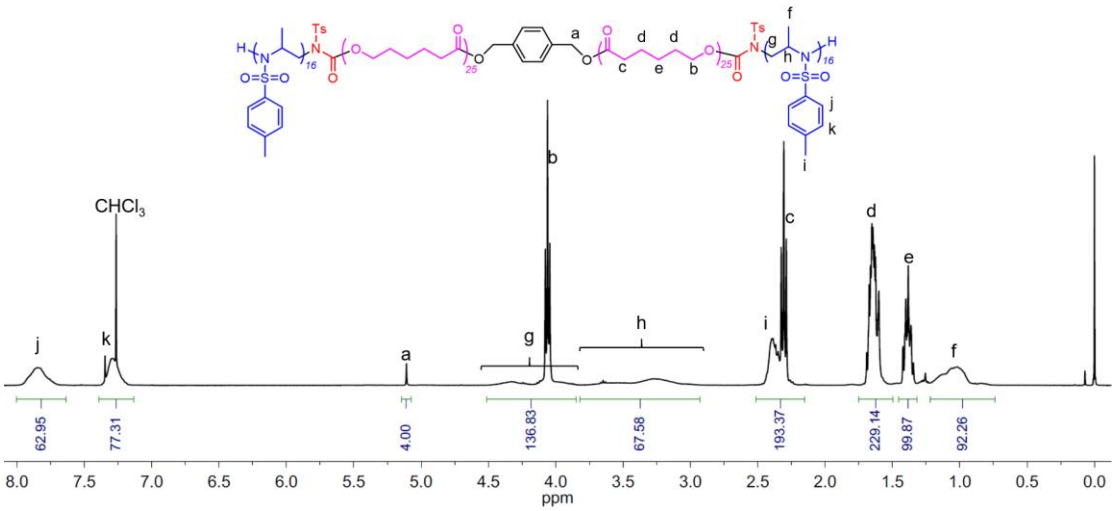

Figure S16. ^{1}H NMR (400 MHz, $CDCl_3$) spectrum of P(TsMAz)$_{16}$-*b*-PCL$_{50}$-*b*-P(TsMAz)$_{16}$ (sample of entry 8, Table 2). The molar mass determined by end-group analysis was calculated as follows: $M_{n,NMR}$ = $MW_{initiator}$ + MW_{TSI} ×2 + MW_{CL} × [(I_e/I_a × 4)/2] + MW_{TsMAz} × [(I_f/I_a × 4)/3], *I*: the integral of the related signal.

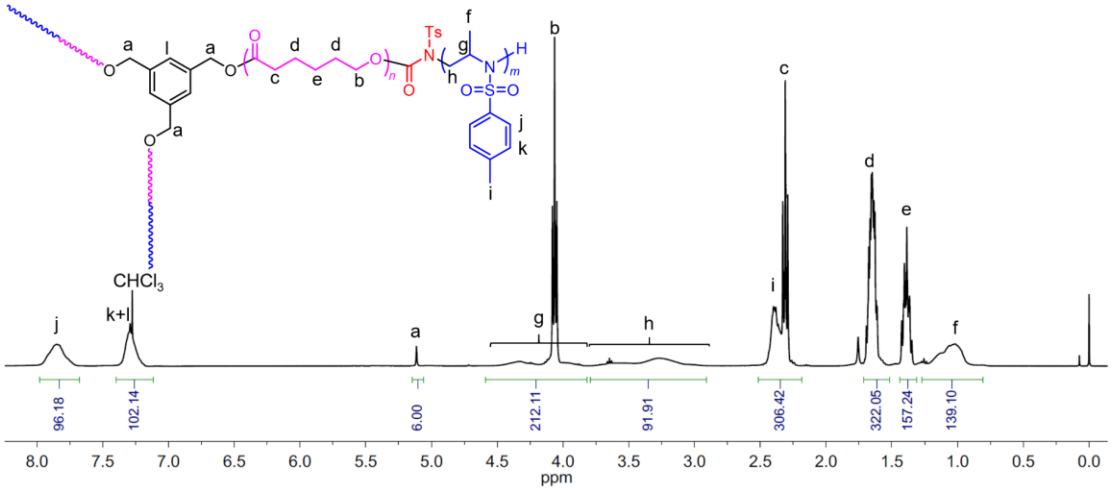

Figure S17. ^{1}H NMR (400 MHz, $CDCl_3$) spectrum of $[PCL_{26}\text{-}b\text{-}P(TsMAz)_{16}]_3$ (sample of entry 9, Table 2). The molar mass determined by end-group analysis was calculated as follows: $M_{n,NMR}$ = $MW_{initiator}$ + MW_{TSI} ×3 + MW_{CL} × $[(I_e/I_a \times 6)/2]$ + MW_{TsMAz} × $[(I_f/I_a \times 6)/3]$, I: the integral of the related signal.

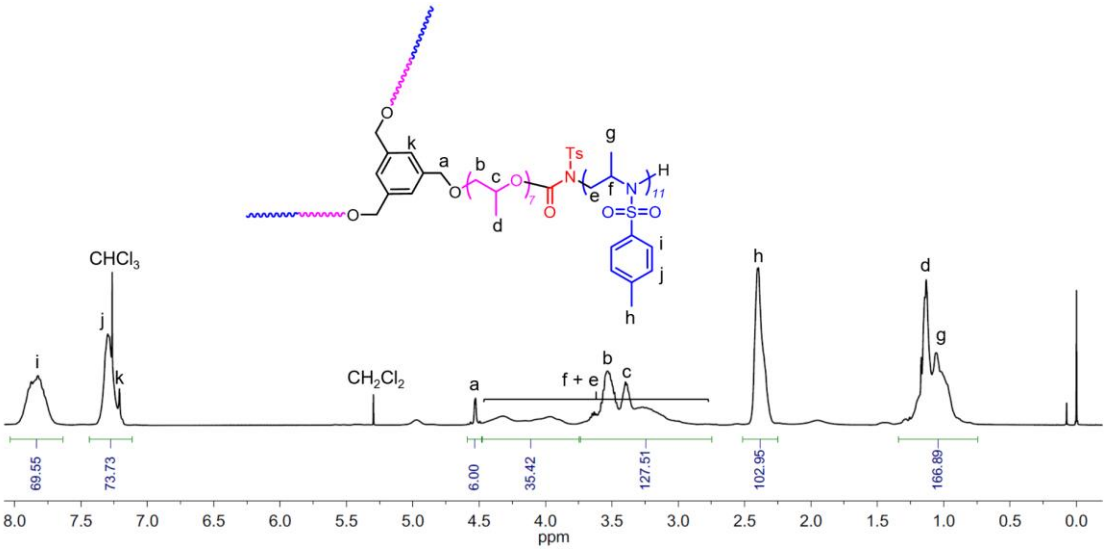

Figure S18. ^{1}H NMR (400 MHz, $CDCl_3$) spectrum of $[PPO_7\text{-}b\text{-}P(TsMAz)_{11}]_3$ (sample of entry 10, Table 2). The molar mass determined by end-group analysis was calculated as follows: $M_{n,NMR}$ = $MW_{initiator}$ + MW_{TSI} ×3 + MW_{PO} × $[(I_d + I_g - I_h)/I_a \times 6]/3$ + MW_{TsMAz} × $[(I_h/I_a \times 6)/3]$, I: the integral of the related signal.

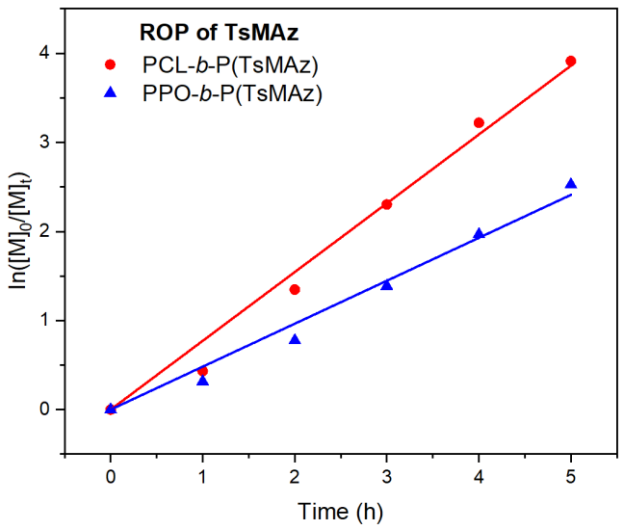

Figure S19. Kinetic plots of $\ln([M]_0/[M]_t)$ versus time for the ROP of TsMAz in their sequential ROP for the synthesis of PCL-*b*-P(TsMAz) and PPO-*b*-P(TsMAz).

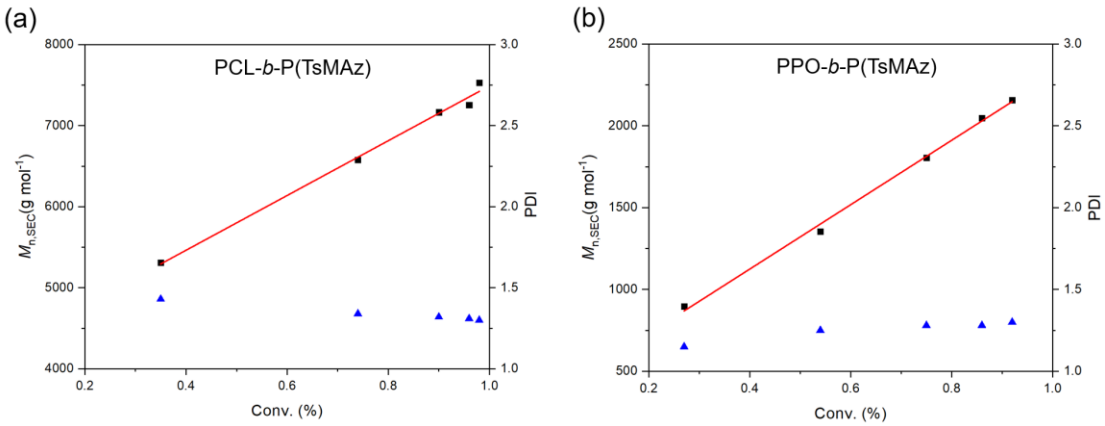

Figure S20. Plots of $M_{n,SEC}$, and $Đ$ versus monomer conversion.

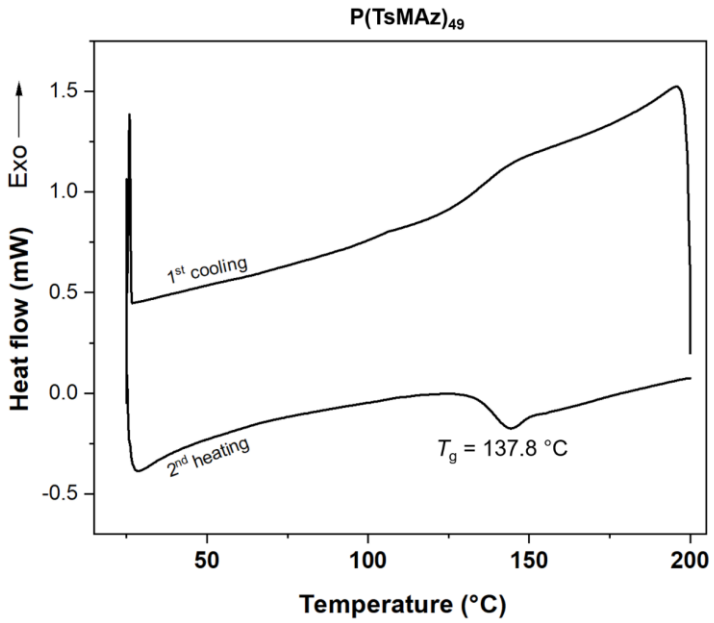

Figure S21. DSC curves (1st (cooling) and 2nd run (heating), 10 °C/min) of $P(TsMAz)_{49}$ (sample of entry 3, Table 1).

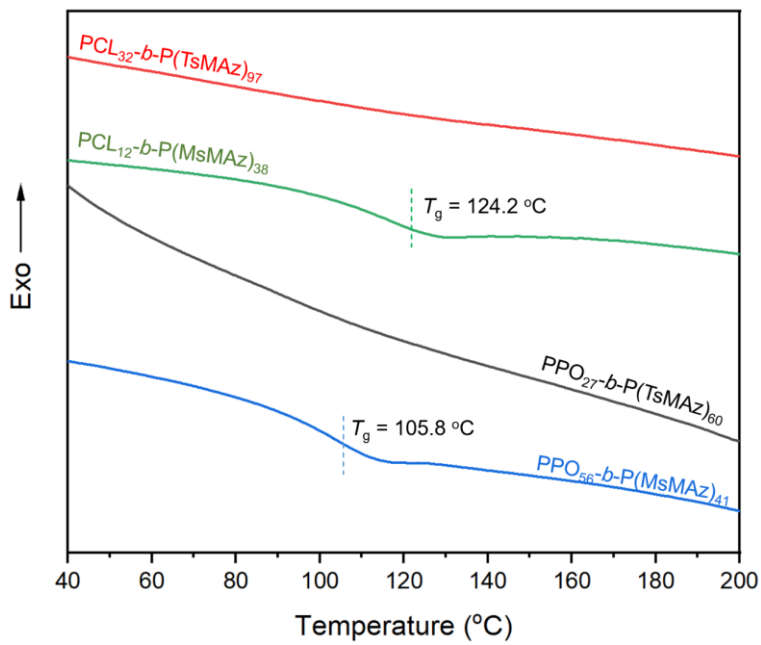

Figure S22. DSC curves (2nd run (heating), 10 °C/min) of representative copolymers.

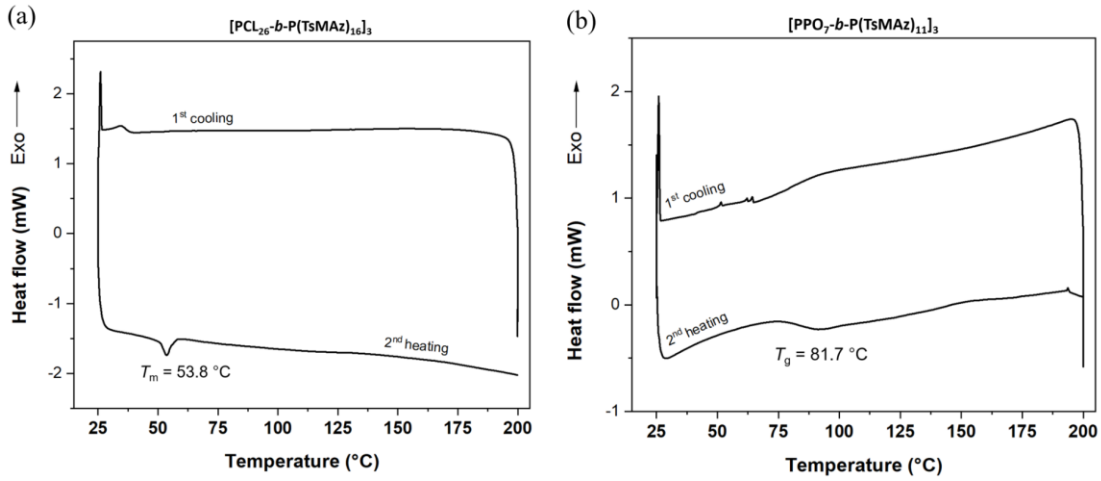

Figure S23. DSC curves (2nd run (heating), 10 °C/min) of representative 3-arm star copolymers.